A Novel Heat Exchanger Effectiveness Approach for Exploring Performance Limits of Two-Phase Mini-Channel Boilers

Felipe Valenzuela, Alfonso Ortega,
Laboratory for Advanced Thermal and Fluids Systems
Department of Mechanical Engineering
Villanova University,
Villanova, PA, USA, 19085
Email: fvalenzu@villanova.edu

ABSTRACT

Indirect two-phase cooling with refrigerants allows management of CPU/GPU heat loads well in excess of those that can be managed with water cooling. Two-phase mini channel boilers are at the heart of such systems. Similar to single-phase cold plates, the performance of mini-channel boilers depends on proper selection of design parameters such as fin pitch, thickness and total surface area that ultimately dictates the number of fins. But unlike single-phase cold plates, two-phase cold plates must also take into account ancillary issues such as boiling flow instabilities, vapor generation and potential loss of coolant that severely affect thermal performance. The traditional metric used in assessing the thermal performance of boilers is thermal resistance, which can be used for comparative studies but does not offer a true assessment of cooling limits. In this paper, we introduce a new definition of heat exchanger effectiveness for two-phase boilers that can be used to compare actual performance to maximum performance and by its definition can also establish cooling limits. We show that the thermal resistance is directly related to the effectiveness. By first maximizing effectiveness, the design thermal resistance can be achieved by the proper sizing of an optimized heat exchanger core. The methodology is first validated for single-phase liquid cold plates by comparing the thermal resistance obtained from the proposed approach to that obtained from the commonly used definition. The proposed approach is demonstrated on experimentally characterized boilers found in the literature. The experimentally determined effectiveness for these test boilers demonstrates the utility of the technique.

KEY WORDS: Electronic cooling, two-phase, evaporators, boilers, effectiveness, NTU, cooling limit.

NOMENCLATURE

A_c	Heatsink fin cross section, m^2
A_{ht}	Total heat transfer area of heatsink, m^2
B	Heatsink width, m
Bo_{max}	Boiler maximum boiling number, -
C	Heat capacity rate, W/K
C_r	Heat capacity rate ratio, -
c_p	Fluid specific heat, J/kg K
D_i	Internal diameter, m
D_o	External diameter, m
h_c	Heat transfer coefficient, W/K m^2
h_{fg}	Difference between saturated vapor and saturated liquid enthalpy, J/kg
H_{ch}	Channel height, m
k	Thermal conductivity, W/K m
L_F	Heatsink fin length, m
L_{ch}	Cold plate channel length, m
N	Number of fins, -
NTU	Number of transfer units, -
Nu_m	Average Nusselt number, -
P	Heatsink fins perimeter, m
Pr	Prandtl number, -
$\dot{Q}_{max}$	Maximum possible heat transfer rate, W
$\dot{Q}''_{chip}$	Heat flux dissipated from electronics, W/m^2
T	Temperature, K
t	Thickness of heatsink fin, m
t_{ch}	Width of heatsink channel, m
t_D	Circular channel wall thickness, m
R	Thermal resistance, K m^2/W
Re	Reynolds number, -
$\forall_{ft}$	Heatsink/cold plate footprint, m^3
w	Heatsink length, m
x_{out}	Boiler exit vapor quality, -

Greek symbols

α	Channel aspect ratio, -
β	Heatsink fin parameter, -
ΔT_{sub}	Inlet subcooling, K
ε	Heat exchanger effectiveness, -
η_F	Heatsink fin efficiency, -

Subscripts

b	Heatsink base
c	Cold-fluid stream
cc	Circular channel
cp	Cold plate
f	fluid
h	Hot-fluid stream
H	Highest
hs	Heatsink
in	Fluid stream inlet
L	Lowest

out	Fluid stream outlet
rc	Rectangular channel
solid	Heatsink / cold plate / boiler
sat	Saturation state
t	Tip of the heatsink fins

INTRODUCTION

Over the last two decades, indirect two-phase cooling has been widely investigated within the electronic cooling community [1-5]. However, the theoretical maximum cooling capability of practical cooling devices such as two-phase cold plates, i.e. boilers, has not been addressed to now. The establishment of such a cooling limit is needed, not only because it aids in determining how much a heatsink design can be improved (material, geometry, etc.), but also because current CPUs, GPUs and TPUs have surpassed air cooling capacity for practical volumetric and acoustic constraints, and are approaching single-phase liquid cooling limits.

The overall thermal performance of an electronic package is determined by the junction to fluid thermal resistance, which includes the thermal resistance due to conduction through the chip, the TIM materials and the heat spreader, as well as the heatsink thermal resistance:

$$R_{hs} = \frac{T_{base} - T_{fluid}}{\dot{Q}} \tag{1}$$

where T_{base} is the heatsink base temperature, T_{fluid} is a reference fluid temperature, selected as the inlet fluid temperature for air-cooled heatsinks and single-phase cold plates, and $\dot{Q}$ is the dissipated heat load. This heatsink thermal metric has been commonly used to evaluate and compare the performance of cooling technologies from air-cooled heatsinks to single-phase cold plates. Hence, for indirect two-phase cooling as a new heat removal technology, R_{hs} would seem to be a reasonable metric to evaluate the performance of two-phase cold plates. But, the physics of two-phase cold plates are more complex than their single-phase counterparts. Flow instabilities, effects of pressure drop on thermal performance, and different flow regimes inside the channels influence the heat transfer during flow boiling and make the definition of a thermal metric such as thermal resistance less obvious [6-8]. Furthermore, in real applications, regions of single-phase heat transfer (sensible heat) and two-phase heat transfer (latent heat) coexist inside these compact heat exchangers and thus the selection of a reference fluid temperature for the thermal resistance is not trivial.

In the literature, the most accepted thermal resistance definition utilizes the coolant inlet temperature [1]. Alternatively, thermal designers have used fluid bulk temperature [9-11], inlet [12, 13] or outlet [14] saturation temperature and average saturation temperature [15-17]. These thermal resistance definitions are often ambiguous as each one ignores different physical effects. This ambiguity in the definition of R_{hs} not only prevents the formulation of cooling limits for two-phase boilers but also introduces significant error and arbitrariness in the use of the common bookkeeping procedure in which total junction to ambient thermal resistance is defined as the sum of the thermal resistances internal and external to the package.

The effectiveness-NTU method, developed by Kays and London [18], has been universally used in heat exchanger design since its introduction [19]. It is a powerful approach that provides a physics basis for optimizing compact heat exchanger performance [18, 20, 21]. The effectiveness of a heat exchanger (ε) compares the actual heat transfer rate to the thermodynamically-limited maximum possible heat transfer rate that could be exchanged between the two fluid streams. Therefore, the $\varepsilon - \mathrm{NTU}$ method not only offers the possibility of establishing a physics-based heat transfer limit for heat exchangers ($\varepsilon = 1$), but also allows direct comparison of the performance of different types of heat exchangers by comparing effectiveness ε for a given NTU value. Because heatsinks and cold plates are ostensibly one-fluid heat exchangers they may be approximately analyzed using traditional heat exchanger approaches. In electronics cooling system design, the $\varepsilon - \mathrm{NTU}$ method has been used for design optimization by considering the heatsink or cold plate to be a metal-to-fluid heat exchanger. Two main approaches can be found in the literature. The first technique, illustrated in an early contribution by Copeland [22], assumes a uniform heatsink wall temperature along the path of the fluid stream. From the standpoint of heat exchanger theory this means that the fluid has a heat capacity rate much lower than that of the metal or that the metal has an infinitely large heat capacity rate ($C_{solid} = \infty$).

Deans et al. [23] developed a second approach, which considers that the fluid and solid have comparable heat capacity rates. This is possible under the assumption that the energy flowing in the heatsink material, usually metal, is treated as an effective second heat exchanger stream. Moreover, a procedure to analytically determine the heat capacity rate of an air-cooled heatsink was defined[1]. Deans's approach thus allows the use of conventional heat exchanger design-theory and procedures for the design of heatsinks and cold plates [18].

Neither approach has been widely adopted, despite their simplicity and their important ramifications in introducing true physics-based performance limits. Copeland's approach has been demonstrated in a few cited studies as a design methodology for air-cooled heatsinks, water-cooled cold plates and electronic cooling modules [24-27]. This approach, however, is not suitable for two-phase cold plates (or boilers) as the boiling fluid also has infinitely large heat capacity rate.

[1] This concept will be fully described during next section

In the present paper, we show that the modeling approach of Dean et al. [23] provides a rigorous physics-based method by which the effectiveness of solid-to-fluid two-phase boilers can be evaluated. A thorough derivation and analysis of the method developed in [23] will first be presented. Then, an extension of the method validation will be carried out for water-cooled cold plates. Finally, the definitions of $Q_{\max}$, NTU and ε for mini-channel boilers are derived, and validation for three different mini boiler models is shown. Of particular interest to this work is developing a method for establishing cooling limits for these types of heat exchangers, and providing a rigorous means for comparing them to other electronic cooling technologies

EFFECTIVENESS ANALYSIS FOR HEATSINKS AND COLD PLATES

Heatsinks and cold plates used in cooling electronic components are fundamentally solid-to-fluid heat exchangers. The traditional analysis of heat exchangers considers fluid-to-fluid heat exchange, from a hot fluid to a cold fluid. Based on an energy balance, Kays and London [18] express the total rate of heat transfer between the hot and cold fluid in two separate equations:

$$\dot{Q} = C_h \left(T_{h,in} - T_{h,out} \right) \tag{2}$$

$$\dot{Q} = C_c \left(T_{c,\,out} - T_{c,\,in} \right) \tag{3}$$

Here, $C = \dot{m} c_p$ for the hot or cold streams, respectively. By this usage, it is understood that the flows transport sensible heat in a single-phase fluid such as a gas or liquid.

In the work of Deans et al. [23], the basic assumption is that a heatsink can be considered to be a solid-to-liquid heat exchanger. Their novel contribution is in showing that the heat flow conducted along the solid can be treated as an equivalent hot-fluid stream. Thus, Eq. 2. can be re-written as:

$$\dot{Q} = C_{solid} \left(T_H - T_L \right) \tag{4}$$

where T_H is the highest temperature and T_L the lowest temperature in the heatsink or cold plate solid material, respectively. The selection of T_H and T_L depends on the geometry of the heatsink, cold-plate or boiler. As shown by Deans et al., for a common straight fin air-cooled heatsink, the highest temperature and the lowest temperature are located at the heatsink base (T_b) and the tip of the fins (T_t). Hence

$$\dot{Q} = C_{solid} \left(T_b - T_t \right) \tag{5}$$

where C_{solid} is the equivalent $\dot{m} c_p$ of the heatsink solid elements [18]. In Eq. 4. $\dot{Q}$ and $\left(T_b - T_t \right)$ are determined using the analytical solution for one-dimensional heat conduction in a fin. Assuming an adiabatic tip, $\dot{Q}$ and $\left(T_b - T_t \right)$ can be expressed as:

$$T_b - T_t = \left(T_b - T_{f,\,in} \right) \left(1 - \frac{1}{\cosh\left(\beta L_F \right)} \right) \tag{6}$$

$$\dot{Q} = N h_c P \tanh(\beta L_F) \frac{T_b - T_{f,\,in}}{\beta} \tag{7}$$

where $\beta = \sqrt{h_c P / k A_c}$, h_c is the heat transfer coefficient, P is the fin perimeter, k is the thermal conductivity of the fin material, A_c is the fin cross section, L_F is the length of the fins and N is the number of fins. By solving for C_{solid} in Eq. 5, one can obtain the equivalent solid heat capacity rate:

$$C_{solid} = \frac{N h_c P}{\beta} \frac{\tanh(\beta L_F)}{1 - \frac{1}{\cosh\left(\beta L_F \right)}} \tag{8}$$

Heat Exchanger Effectiveness

The heat exchanger effectiveness is a performance metric that compares the actual heat exchanged to the maximum theoretical heat exchange for the given flow rates and inlet temperatures in a heat exchanger. With the introduction of the concept of effective flow in the solid given by Eq. 5, we can write:

$$\varepsilon = \frac{\dot{Q}}{\dot{Q}_{max}} = \frac{C_{solid} \left(T_b - T_t \right)}{C_{min} \left(T_b - T_{f,\,in} \right)} = \frac{C_f \left(T_{f,\,out} - T_{f,\,in} \right)}{C_{min} \left(T_b - T_{f,\,in} \right)} \tag{9}$$

where C_{min} is the smaller of the C_{solid} and C_f magnitude. Clearly the maximum theoretical value of effectiveness is 1.0 when the actual heat rejected reaches the theoretical maximum.

Heat Exchanger Number of Transfer Units

The number of transfer units, NTU, is a non-dimensional grouping that naturally occurs in the theoretical analysis of the thermal performance of a heat exchanger. For a solid-to-fluid heat exchanger, it is defined as:

$$\mathrm{NTU} = \frac{h_c A_{ht}}{C_{min}} \tag{10}$$

where $h_c A_{ht}$ is the overall heat transfer coefficient (UA) for a solid-to-fluid heat exchanger. Unlike fluid-to-fluid heat exchangers, it only considers the cold-side heat transfer coefficient. Hence, A_{ht} is the total surface area of the heatsink that is involved in transferring heat to the fluid side.

Heat Capacity Ratio

The heat capacity ratio is defined as:

$$C_r = \frac{C_{min}}{C_{max}} \tag{11}$$

where C_{max} is the larger of the C_{solid} and C_f magnitude.

Effectiveness of Straight Fin Heatsinks

For any heat exchanger, ε is a function of NTU, C_r and the flow arrangement [18]. The flow arrangement of a solid-to-fluid heat exchanger can be determined by analyzing the relative direction of the heat flow conducted along the fins with respect to the direction of the coolant stream. The effectiveness of this type of heat exchanger can thus be determined using the well-known effectiveness-NTU relations for compact heat exchangers [18, 20, 21] that are well documented for different flow arrangements. Under the assumption of an isothermal heatsink base and homogeneous fins, Deans et al. [23] established that a straight fin air-cooled heatsink behaves as a crossflow heat exchanger with both fluids mixed (Figure 1.). For this case the relationship is given by [18]:

$$\varepsilon_{hs} = \frac{\mathrm{NTU}}{\frac{\mathrm{NTU}}{1-e^{-\mathrm{NTU}}} + \frac{C_r \cdot \mathrm{NTU}}{1-e^{-C_r \cdot \mathrm{NTU}}} - 1} \tag{12}$$

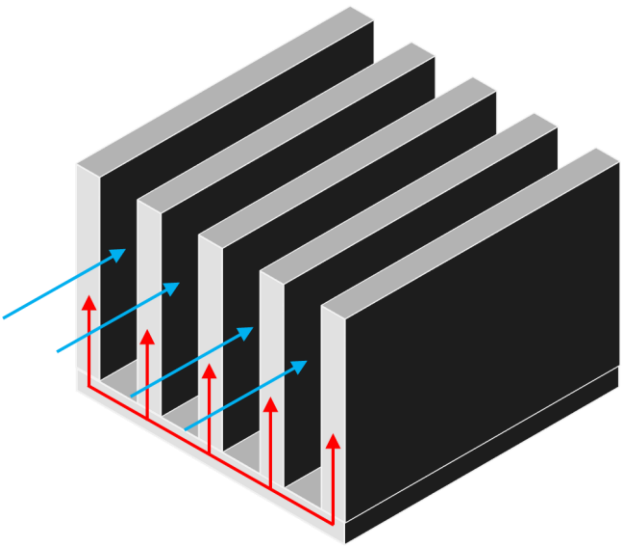

Fig.1 Flow arrangement diagram for a straight fin air-cooled heatsink

Effectiveness-Thermal Resistance Relation

The relationship between ε and R_{hs} can be found by re-writing Eq. 9. as:

$$\dot{Q} = \varepsilon\, C_{min}\left(T_b - T_{f,in}\right) \tag{13}$$

and defining R_{hs} (Eq. 1.) in terms of the fluid inlet temperature

$$R_{hs} = \frac{T_b - T_{f,in}}{\dot{Q}} \tag{14}$$

Thus by combining Eq. 13. and 14:

$$R_{hs} = \frac{1}{\varepsilon\, C_{min}} \tag{15}$$

APPLICATION OF EFFECTIVENESS-NTU ANALYSIS FOR SINGLE PHASE COLDPLATES

In this section, as an extension of the validation presented by Deans et al. [23] for air-cooled heatsinks, three case studies of water-cooled cold plates were analyzed. The thermal resistance obtained using the $\varepsilon - R_{hs}$ relation (Eq. 15.) was compared to the commonly used thermal resistance definition (Eq. 14.). The effectiveness of the cold plates was obtained by using the effectiveness-NTU relation corresponding to the flow arrangement, which depends on the direction of the heat flow conducted through the solid relative to the water flow direction. For the first two cases, circular and rectangular single channels, the cold plate base temperature was computed using the analytical solution of the solid heat conduction. On the other hand, for the multi-channel cold plate studied by Lei [28], the base temperature was obtained from the reported experimental data. All the analyzed cases consider fixed cold plate dimensions with a variable water flow rate.

Circular Channel

The circular channel is made of copper and has an internal diameter D_i, length L_{ch} and wall thickness t_D of 5mm, 50mm and 2mm, respectively. A uniformly distributed 10W heat load over the channel external surface area was applied. Water enters at six different flow rates with an inlet temperature of 22°C. It can be shown that by analytically solving the heat conduction of a circular channel and replicate the procedure from Eq. 2. to Eq. 8. the circular channel heat capacity rate is obtained:

$$C_{solid} = \frac{2\pi k\, L_{ch}}{\ln(D_o / D_i)} \tag{16}$$

where k is the thermal conductivity, L_{ch} is the channel length and $D_o = D_i + 2t_D$ is the channel external diameter. Due to the way in which the heat is applied to the channel, the best flow arrangement representing the case study is shell-and-tube. Hence the effectiveness-NTU relation [18] for the circular channel is given by

$$\varepsilon_{cc} = \frac{2}{1 + C_r + \sqrt{1 + C_r^2}\,\dfrac{1 + e^{-\Gamma}}{1 - e^{-\Gamma}}} \tag{17}$$

where

$$\Gamma = NTU\sqrt{1 + C_r^2} \tag{18}$$

The heat transfer coefficient needed to compute NTU is determined using a simultaneously developing Nusselt number correlation for circular ducts [29]:

$$\mathrm{Nu}_{m,cc} = \frac{1}{4x^*}\ln\left[\frac{1}{1 - 2.654(x^*)^{0.5}\,\mathrm{Pr}^{-0.167}}\right] \tag{19}$$

where

$$x^* = \frac{L_{ch}}{D_i\,\mathrm{Re}\,\mathrm{Pr}} \tag{20}$$

where Re and Pr are Reynolds number and Prandtl number, respectively. Finally, by replacing Eq. 17. into Eq. 15. the circular mini-channel thermal resistance is obtained

$$R_{cc} = \frac{1}{C_{min}\,\varepsilon_{cc}} \tag{21}$$

Figure 2. shows the variation of circular mini-channel thermal resistance (Eq. 21.) with respect to the water flow rate. These results were compared with the single-phase thermal resistance (Eq. 14.) obtaining less than a 1% relative error for the entire flow rate range (Figure 3.). In this case study, for the first three flow rates C_{min} corresponded to the coolant $\dot{m}c_p$, whereas for the last three flow rates C_{min} corresponded to C_{solid}.

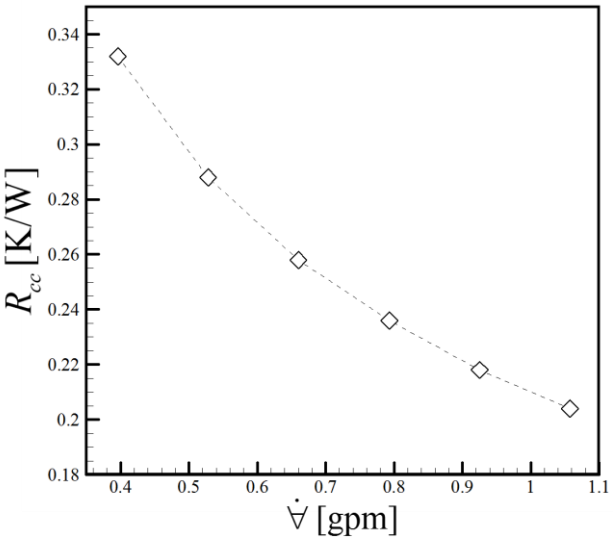

Fig.2 Circular mini-channel thermal resistance v/s water flow rate

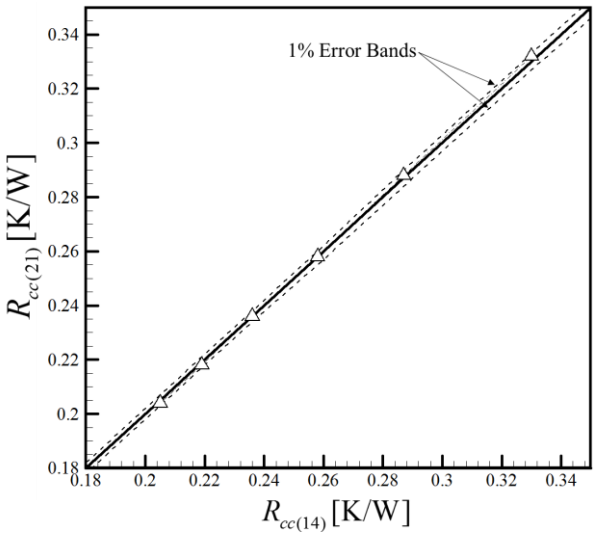

Fig.3 Comparison of obtained thermal resistance with Eq. 14. for a circular mini-channel

Rectangular Channel

The copper rectangular channel is 50mm long, 6mm high and 2mm wide. The channel wall thickness is 2mm. A 10W heat load was uniformly applied to the channel base. Both sidewalls, as well as the top of the channel, are insulated. 22°C water enters the channel at six different flow rates. In order to obtain both the analytical solution of heat conduction and the solid heat capacity rate, the rectangular channel is modeled as a finned heatsink. Hence, C_{solid} is computed using Eq. 8. and the channel effectiveness is given by Eq. 12:

$$\varepsilon_{rc} = \frac{\mathrm{NTU}}{\dfrac{\mathrm{NTU}}{1 - e^{-\mathrm{NTU}}} + \dfrac{C_r \cdot \mathrm{NTU}}{1 - e^{-C_r \cdot \mathrm{NTU}}} - 1} \tag{22}$$

In this case, $NTU = h_c A_t / C_{min}$, where $A_t = 2L_{ch}H_{ch}$ and H_{ch} is the channel height. h_c is computed using the Nusselt number correlation proposed by Stephan for flat gaps [30]:

$$Nu_{m,rc} = 7.55 + \frac{0.024(x^*)^{-1.14}}{1 + 0.0358(x^*)^{-0.064}\,\mathrm{Pr}^{0.17}} \tag{23}$$

where x^* is also given by Eq. 20. Thus, Eq. 15. can be written as:

$$R_{rc} = \frac{1}{C_{min}\varepsilon_{rc}} \tag{24}$$

Figure 4. depicts the obtained thermal resistance against the water flow rate variation. A maximum relative error of 1.79% was achieved when compared to the well-known thermal resistance definition (Figure 5.). For the entire flow rate range C_{min} corresponded to C_{solid}.

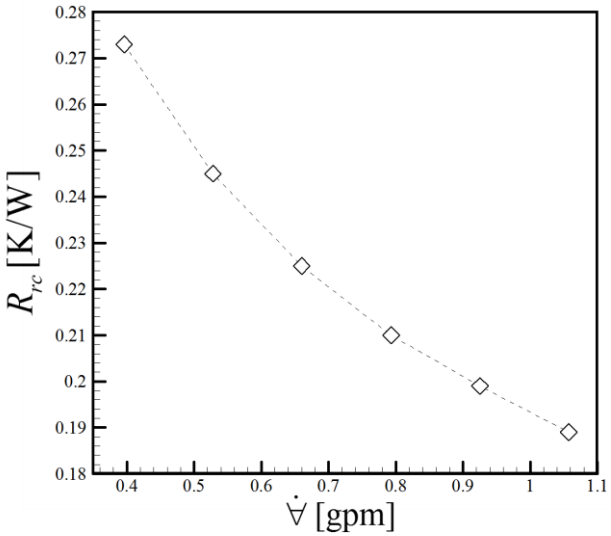

Fig.4 Rectangular mini-channel thermal resistance v/s water flow rate

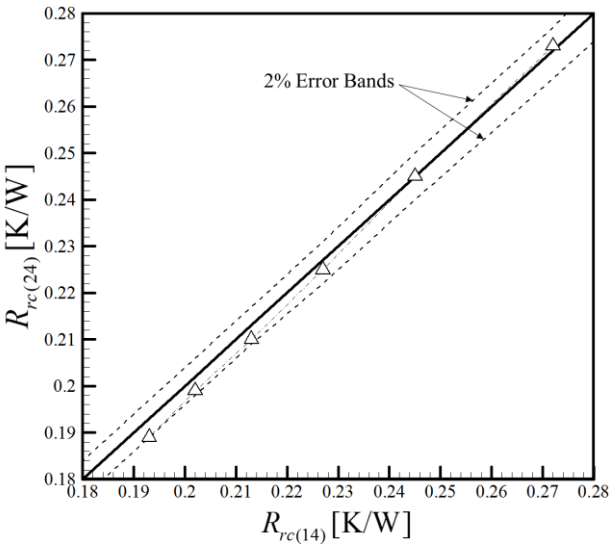

Fig.5 Comparison of obtained thermal resistance with Eq. 14. for a rectangular mini-channel

Multi-Channel Cold Plate

The copper single-layer cold plate studied by Lei [28] is 12.7mm wide and 30.5mm long and has eight 0.508mm × 0.508mm square channels. The separation between each channel and the thickness of the cold plate base are 1.016mm and 0.508mm, respectively. Water at 23ºC was supplied at six different flow rates, from 100 to 600 mL/min. Only the center portion of the cold plate (25.4mm × 12.7mm) was directed heated with 80W. Because the wall thickness is twice the channel width, the multi-channel cold plate cannot be modeled as a finned heatsink. Therefore, the solid temperature difference, needed to obtain the cold plate heat capacity rate, was obtained as follows:

1. The channel base temperature was computed using both the reported cold plate base temperature and one-dimensional heat conduction through the copper.

2. The channel top temperature is determined using the mini-channel energy balance approach proposed by Qu and Muduwar [31], where the heat transfer coefficient is obtained by correcting the parallel plate correlation (Eq. 23.) with a correction factor for a rectangular channel of finite aspect ratio [18]:

$$Nu_{m,sc} = Nu_{m,rc} \cdot G(\alpha) \tag{25}$$

$$G(\alpha) = 1 - 2.04\alpha + 3.08\alpha^2 - 2.47\alpha^3 + 1.05\alpha^4 - 0.18\alpha^5 \tag{26}$$

where α is the channel aspect ratio. Finally, the cold plate top temperature (T_t) is determined by one-dimensional heat conduction between the channel top and the cold plate top. Hence, the cold plate heat capacity rate for each case as:

$$C_{solid} = \frac{\dot{Q}}{T_b - T_t} \tag{27}$$

The cold plate effectiveness is determined using the crossflow heat exchangers-both fluids mixed effectiveness NTU relation:

$$\varepsilon_{cp} = \frac{\text{NTU}}{\dfrac{\text{NTU}}{1-e^{-\text{NTU}}} + \dfrac{C_r \cdot \text{NTU}}{1-e^{-C_r \cdot \text{NTU}}} - 1} \tag{28}$$

Finally, the cold plate thermal resistance can be determined using Eq. 15. as:

$$R_{cp} = \frac{1}{C_{min}\varepsilon_{cp}} \tag{29}$$

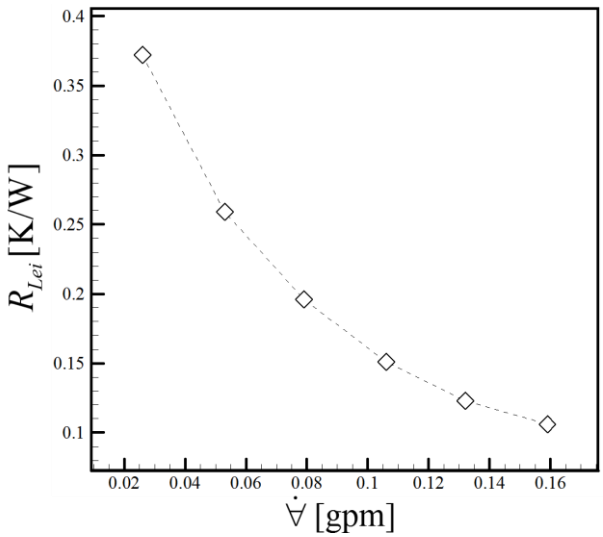

Fig.6 Reported cold plate thermal resistance from Lei [28] v/s water flow rate

Figure 6. shows the cold plate thermal resistance reported in Lei [28]. The thermal resistance comparison between the experimental work developed by Lei and the proposed approach resulted in a maximum 1.04% relative error (Figure 7.). The studied cold plate C_{min} corresponded to $\dot{m}c_p$ under the selected flow rates.

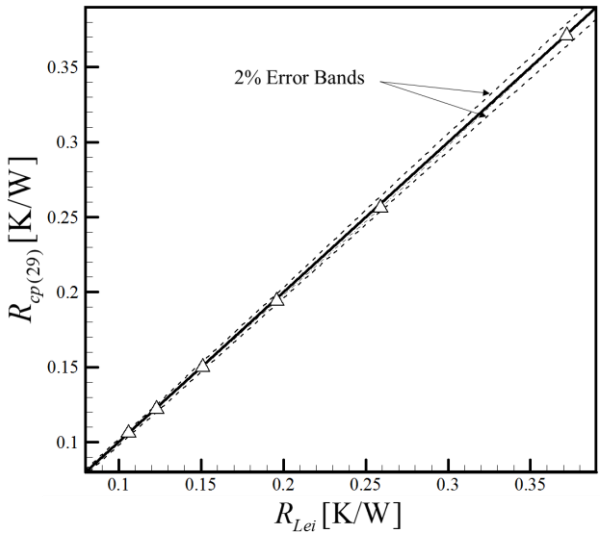

Fig.7 Comparison of obtained cold plate thermal resistance with reported thermal resistance by Lei [28]

EFFECTIVENESS-NTU ANALYSIS FOR SOLID-TO-FLUID BOILERS

If in a solid-to-fluid heat exchanger the fluid experiences boiling, its temperature remains approximately constant along the channels, while the solid encounters a temperature drop from the base to the tip of the fins. This effect implies that $C_f >> C_{solid}$ or $C_f \to \infty$. For this limiting case, regardless of the boiler flow arrangement, NTU and ε are given by Eq. 30 and 31, respectively.

$$NTU = \frac{h_c A_{hs}}{C_{solid}} \tag{30}$$

$$\varepsilon = 1 - e^{-NTU} \tag{31}$$

Additionally, considering the steady state assumption of the heat exchanger theory [18], the heat flow exchanged between the solid and the fluid is equal to the heat dissipated from the electronics ($\dot{Q}$). Thus, the effectiveness of a solid-to-fluid boiler is defined as:

$$\varepsilon = \frac{\dot{Q}}{C_{solid}\left(T_b - T_{f,in}\right)} \tag{32}$$

Although the effectiveness-NTU relation for a boiler is not geometry dependent, both NTU (Eq. 30.) and ε (Eq. 31.) are functions of C_{solid}, which depends on geometrical and material parameters of the solid-to-liquid heat exchanger. For example, combining Eq. 8. and Eq. 30. the number of transfer units is given by

$$NTU = \frac{1}{\eta_F}\left[1 - \frac{1}{\cosh(\beta L_F)}\right] \tag{33}$$

where η_F is the fin efficiency defined as:

$$\eta_F = \frac{\tanh(\beta L_F)}{\beta L_F} \tag{34}$$

Maximum Performance of Solid-to-Fluid Boiler

By determining C_{solid} and using the infinitely long counterflow heat exchanger concept, the proposed approach can be used to compute the thermodynamically-limited maximum possible heat transfer rate for any solid-to-fluid two-phase boiler. For a given T_b and $T_{f,in}$

$$\dot{Q}_{max} = C_{solid}\left(T_b - T_{f,in}\right) \tag{35}$$

It is important to note that the maximum temperature gradient (ΔT_{max}) has been defined in terms of the inlet fluid temperature instead of the saturation temperature. This allows capturing the sensible heat effect on the performance when the fluid enters at a subcooled state. Intuitively, $\dot{Q}_{max}$ can be increased by increasing $T_b - T_{f,in}$. However, in order to keep a large temperature gradient throughout the entire evaporator, the subcooling level ($\Delta T_{sub} = T_{sat} - T_{f,in}$) should be as small as possible. Thus, a more effective way to increase ΔT_{max} is by reducing T_{sat} .

In a conventional fluid-to-fluid boiler the maximum heat transfer rate can be achieved in a counterflow heat exchanger of infinite length when $T_{h,in} = T_{sat}$ ($T_t = T_{sat}$ for a solid-to-fluid). However, this result does not yield useful constraints on the boiling fluid. Instead, in order to determine the outlet condition of the boiling fluid when the maximum heat transfer rate is achieved in a solid-to-fluid boiler, we first assume that the fluid never reaches its superheated state:

$$\dot{m}c_p \Delta T_{sub} + \dot{m}h_{fg} < \dot{Q}_{max} \tag{36}$$

Thus, the maximum heat transfer rate is achieved when in an infinitely long counterflow boiler the fluid exit quality is

$$x_{\max} = \frac{C_{solid}\left(T_b - T_{f,in}\right) - \dot{m} c_p \Delta T_{sub}}{\dot{m} h_{fg}} \tag{37}$$

Equivalently, when no subcooling is allowed, the fluid exit quality when the maximum heat transfer rate is achieved can be written as

$$x_{\max} = \frac{\dot{Q}_{max}}{\dot{m} h_{fg}} = Bo_{max} \tag{38}$$

APPLICATION OF EFFECTIVENESS-NTU ANALYSIS FOR SOLID-TO-FLUID BOILERS

The proposed approach was used to determine the effectiveness of three solid-to-fluid two-phase boilers found in the literature. As a validation of the proposed method for each one of the case studies the effectiveness obtained from Eq. 31. was compared with the definition in Eq. 32. The heat transfer coefficient of each experimental data was determined using the mini-channel energy balance approach proposed by Qu and Muduwar [31] .

Ortega et al. [32] performed two-phase flow experiments on the same single-layer cold plate described in the single-phase validation section [28]. 23ºC water was supplied at 20 mL/min, which given the experiment conditions results in a $\Delta T_{sub} \approx 74^o\mathrm{C}$. Although the heat input was from 20W to 554W, for this analysis only the heat input providing full saturation at the exit were selected (126W-554W). As can be seen in Table 1., for all the selected data points effectiveness of the studied cold plate was lower than 3.7%. These results are due to the large subcooling condition prescribed at the inlet. The comparison between the effectiveness definition from Eq. 31 and 32 showed a relative error lower than 2.4% for all the studied heat fluxes.

The effectiveness of two open microchannels boilers, one with a uniform manifold [33] and the other with a dual-tapered manifold [34], was also determined. In both designs, the manifold height is larger than the microchannels for the entire microchannel length. This means that the tip of the fins are in contact with the fluid, and thus, C_{solid} has to consider convective tips. Hence, using the same procedure as Deans et al. [23], but adopting convective tip boundary condition for $\dot{Q}$ instead, the solid heat capacity rate can be written as:

$$C_{solid} = N\sqrt{k A_c h_c P}\left(\sinh \beta H + \frac{h_c}{\beta \cdot k}\cosh \beta H\right) \tag{39}$$

The heat flux for the uniform manifold open microchannel boiler studied by Kalani and Kandlikar [33] was varied from 130W/cm^2 to 283W/cm^2. Degassed distilled water was supplied into the boiler with an inlet subcooling of 10ºC. With these conditions, the boiler design achieved maximum effectiveness of 59.5% (Table 2.). Although a good agreement between the results from Eq. 31 and 32 was found, a maximum relative error of 11.75% was encountered for the lowest heat flux. This relative larger error is due to the heat transfer coefficient error associated with the larger sensible heat observed in the lowest heat flux.

The open microchannels boiler with symmetric dual tapered manifold was studied by Chauhan and Kandlikar [34] as part of a thermosyphon cooling solution for data center CPUs. For the analyzed cases the heat input varied from 4.2W/cm^2 to 18.1W/cm^2. The HFE7000 refrigerant enters the boiler at around $\Delta T_{sub} = 5^o\mathrm{C}$ for all tested cases. The top-bench tests resulted in maximum effectiveness of 63.1% (Table 3.). The relative error was kept under 9% for all the data points. These comparatively high relative errors are associated with the estimation of the heat transfer coefficient and the total heat transfer area.

As expected the effectiveness of the three analyzed boilers was a function of the operation conditions. Although in each case study both the geometry and the flow rate were maintained during the tests, the small variation in the effectiveness was caused by the different heat flux and its associated heat transfer coefficient.

Table 1. Effectiveness of Ortega et al. [32]

$\varepsilon_{(31)}[-]$	$\varepsilon_{(32)}[-]$	$\dot{Q}''[\mathrm{W/cm^2}]$	Relative error [%]
0.031	0.030	95	2.39
0.031	0.031	102	2.38
0.032	0.032	108	2.36
0.033	0.032	114	2.34
0.034	0.033	124	2.32
0.035	0.034	133	2.30
0.037	0.036	143	2.25

Table 2. Effectiveness of Kalani and Kandlikar [33]

$\varepsilon_{(31)}[-]$	$\varepsilon_{(32)}[-]$	$\dot{Q}''[\mathrm{W/cm^2}]$	Relative error [%]
0.595	0.674	130	11.75
0.579	0.597	198	3.05
0.574	0.576	241	0.32
0.573	0.569	283	0.54

Table 3. Effectiveness of Chauhan and Kandlikar [34]

$\varepsilon_{(31)}[-]$	$\varepsilon_{(32)}[-]$	$\dot{Q}''$[W/cm^2]	Relative error [%]
0.631	0.647	4.20	2.43
0.631	0.647	6.19	2.43
0.630	0.632	8.52	0.27
0.630	0.600	11.3	4.91
0.629	0.590	14.4	6.61
0.628	0.577	18.1	8.99

CONCLUSIONS

A novel approach to determine the performance of solid-to-liquid two-phase boilers was developed. This method is based on both the well-known effectiveness-NTU design procedure and the concept of the solid equivalent heat capacity rate developed by Deans et al. [23]. The significant contribution of the proposed methodology is the establishment of a physics cooling limit by defining the thermodynamically-limited maximum possible heat transfer rate for a solid-to-liquid two-phase boiler. Furthermore, the determination of the effectiveness of a solid-to-liquid boiler provides a precise means for comparison to other cooling technologies.

As a demonstration of Deans methodology, a water-cooled cold plate validation was first performed. The validation for solid-to-fluid boiler was carried out by comparing $\varepsilon = 1 - \exp[-NTU]$ to the effectiveness definition based on the proposed theoretical maximum heat transfer rate. The results obtained from both procedures have a good agreement between them demonstrating the accuracy and utility of the developed approach.

ACKNOWLEDGMENT

This material is based upon the work supported by the national Science Foundation Center for Energy Smart Electronic System (ES2) under the Grant No. IIP-1738782. Any opinions, findings, and conclusions or recommendations expressed in this material are those of the author(s) and do not necessarily reflect the views of the National Science Foundation.

REFERENCES

[1] B. Agostini, M. Fabbri, J. E. Park, L. Wojtan, J. R. Thome, and B. Michel, "State of the art of high heat flux cooling technologies," *Heat Transfer Engineering,* vol. 28, pp. 258-281, 2007.

[2] S. G. Kandlikar, "High flux heat removal with microchannels—a roadmap of challenges and opportunities," *Heat Transfer Engineering,* vol. 26, pp. 5-14, 2005.

[3] J. R. Thome, "Micro-Two-Phase Electronics Cooling: Finally on Its Way," in *2019 18th IEEE Intersociety Conference on Thermal and Thermomechanical Phenomena in Electronic Systems (ITherm)*, 2019, pp. 1354-1363.

[4] I. Mudawar, "Assessment of high-heat-flux thermal management schemes," *IEEE Transactions on Components and Packaging Technologies,* vol. 24, pp. 122-141, 2001.

[5] M. K. Sung and I. Mudawar, "Single-phase and two-phase hybrid cooling schemes for high-heat-flux thermal management of defense electronics," *Journal of Electronic Packaging,* vol. 131, p. 021013, 2009.

[6] S. G. Kandlikar, "Two-phase flow patterns, pressure drop, and heat transfer during boiling in minichannel flow passages of compact evaporators," *Heat Transfer Engineering,* vol. 23, pp. 5-23, 2002.

[7] J. R. Thome, "State-of-the-art overview of boiling and two-phase flows in microchannels," *Heat transfer engineering,* vol. 27, pp. 4-19, 2006.

[8] G. Wang, P. Cheng, and A. Bergles, "Effects of inlet/outlet configurations on flow boiling instability in parallel microchannels," *International Journal of Heat and Mass Transfer,* vol. 51, pp. 2267-2281, 2008.

[9] R. Chu, R. Simons, and G. Chrysler, "Experimental investigation of an enhanced thermosyphon heat loop for cooling of a high performance electronics module," in *Fifteenth Annual IEEE Semiconductor Thermal Measurement and Management Symposium (Cat. No. 99CH36306)*, 1999, pp. 1-9.

[10] J. Lee and I. Mudawar, "Low-temperature two-phase microchannel cooling for high-heat-flux thermal management of defense electronics," *IEEE transactions on components and packaging technologies,* vol. 32, pp. 453-465, 2009.

[11] B. Pulvirenti, A. Matalone, and U. Barucca, "Boiling heat transfer in narrow channels with offset strip fins: Application to electronic chipsets cooling," *Applied Thermal Engineering,* vol. 30, pp. 2138-2145, 2010.

[12] P. Wang, P. McCluskey, and A. Bar-Cohen, "Two-phase liquid cooling for thermal management of IGBT power electronic module," *Journal of Electronic Packaging,* vol. 135, p. 021001, 2013.
[13] M. Schultz, F. Yang, E. Colgan, R. Polastre, B. Dang, C. Tsang*, et al.*, "Embedded two-phase cooling of large three-dimensional compatible chips with radial channels," *Journal of Electronic Packaging,* vol. 138, p. 021005, 2016.
[14] Y. F. Maydanik, S. V. Vershinin, M. A. Korukov, and J. M. Ochterbeck, "Miniature loop heat pipes-a promising means for cooling electronics," *IEEE Transactions on Components and Packaging Technologies,* vol. 28, pp. 290-296, 2005.
[15] R. Singh, A. Akbarzadeh, C. Dixon, M. Mochizuki, and R. R. Riehl, "Miniature loop heat pipe with flat evaporator for cooling computer CPU," *IEEE transactions on components and packaging technologies,* vol. 30, pp. 42-49, 2007.
[16] C.-C. Chang, S.-C. Kuo, M.-T. Ke, and S.-L. Chen, "Two-phase closed-loop thermosyphon for electronic cooling," *Experimental Heat Transfer,* vol. 23, pp. 144-156, 2010.
[17] P. E. Tuma, "Evaporator/Boiler design for thermosyphons utilizing segregated hydrofluoroether working fluids," in *Twenty-Second Annual IEEE Semiconductor Thermal Measurement And Management Symposium*, 2006, pp. 69-77.
[18] W. Kays and A. London 2nd, "Compact Heat Exchangers, 2nd McGraw-Hill," *New York,* 1964.
[19] T. L. Bergman, F. P. Incropera, D. P. DeWitt, and A. S. Lavine, *Fundamentals of heat and mass transfer*: John Wiley & Sons, 2011.
[20] R. K. Shah and D. P. Sekulic, *Fundamentals of heat exchanger design*: John Wiley & Sons, 2003.
[21] A. Pignotti and R. Shah, "Effectiveness-number of transfer units relationships for heat exchanger complex flow arrangements," *International journal of heat and mass transfer,* vol. 35, pp. 1275-1291, 1992.
[22] D. Copeland, "Optimization of parallel plate heatsinks for forced convection," in *Sixteenth Annual IEEE Semiconductor Thermal Measurement and Management Symposium (Cat. No. 00CH37068)*, 2000, pp. 266-272.
[23] J. Deans, J. Neale, W. Dempster, and C. Lee, "The use of effectiveness concepts to calculate the thermal resistance of parallel plate heat sinks," *Heat transfer engineering,* vol. 27, pp. 56-67, 2006.
[24] D. W. Copeland, "Fundamental performance limits of heatsinks," *TRANSACTIONS-AMERICAN SOCIETY OF MECHANICAL ENGINEERS JOURNAL OF ELECTRONIC PACKAGING,* vol. 125, pp. 221-225, 2003.
[25] R. J. Moffat, "Modeling air-cooled heat sinks as heat exchangers," in *Twenty-Third Annual IEEE Semiconductor Thermal Measurement and Management Symposium*, 2007, pp. 200-207.
[26] R. L. Webb, "Heat exchanger design methodology for electronic heat sinks," *Journal of heat transfer,* vol. 129, pp. 899-901, 2007.
[27] M. J. Ellsworth and L. A. Campbell, "Theoretical (Ideal) Module Cooling and Module Cooling Effectiveness," in *ASME 2015 International Technical Conference and Exhibition on Packaging and Integration of Electronic and Photonic Microsystems collocated with the ASME 2015 13th International Conference on Nanochannels, Microchannels, and Minichannels*, 2015.
[28] N. Lei, "The thermal characteristics of multilayer minichannel heat sinks in single-phase and two-phase flow," *PhD. Dissertation, Mech. Engineering Graduate College, University of Arizona,* 2006.
[29] R. K. Shah and A. L. London, *Laminar flow forced convection in ducts: a source book for compact heat exchanger analytical data*: Academic press, 2014.
[30] K. Stephan, "Wärmeübergang und Druckabfall bei nicht ausgebildeter Laminarströmung in Rohren und in ebenen

Spalten," *Chemie Ingenieur Technik,* vol. 31, pp. 773-778, 1959.
[31] W. Qu and I. Mudawar, "Transport phenomena in two-phase micro-channel heat sinks," *J. Electron. Packag.,* vol. 126, pp. 213-224, 2004.
[32] A. Ortega, N. Lei, and R. Vaidyanathan, "High-Performance Heat Sinks Utilizing Two-Phase Flow in Stacked Minichannels," *Journal of Enhanced Heat Transfer,* vol. 21, 2014.
[33] A. Kalani and S. G. Kandlikar, "Evaluation of pressure drop performance during enhanced flow boiling in open microchannels with tapered manifolds," *Journal of Heat Transfer,* vol. 136, p. 051502, 2014.
[34] A. Chauhan and S. G. Kandlikar, "Characterization of a dual taper thermosiphon loop for CPU cooling in data centers," *Applied Thermal Engineering,* vol. 146, pp. 450-458, 2019.